Pergamon

Journal of Structural Geology, Vol. 17, No. 7. pp. 1055 to 1063, 1995

0191-8141/95 $9.50 + 0.00

0191-8141(94)00130-8

Experimental folding and boudinage under pure constrictional conditions

GUSTAV KOBBERGER

Department of Volcanology, GEOMAR, Wischhofstraße 1-3, D 24148 Kiel, Germany

and

GERNOLD ZULAUF

Geologisch-Paläontologisches Institut der Johann-Wolfgang-Goethe Universität, Senckenberganlage 32-34, D 60054 Frankfurt a.M., Germany

(*Received* 6 *January* 1994; *accepted in revised form* 16 *November* 1994)

Abstract—Constrictional folds are characterized by true fold-axis parallel extension if the rock-volume does not vary during deformation. Studies of such folds in experiments, using plasticine layers of different apparent viscosity and power-law exponent, clearly indicate that fold-axis parallel stretch may be accompanied by plastic elongation as well as boudinage of the competent layer. Characteristic aspects of the experimentally folded competent layers are: (1) coeval development of folds and boudins; (2) layer thickness not changing during deformation; (3) layer-parallel shortening in sections perpendicular to the fold (stretching) axis; (4) enlargement of the initial thickness of the competent layer results in increasing fold wavelength and decreasing number of boudins. The ratio of dominant wavelength to layer thickness of the constrictional folds can be described mathematically approximately by the equation developed for plane strain folding of power-law materials.

INTRODUCTION

Folds with axis-parallel extension are common in various types of naturally deformed rocks. Extension parallel to the fold axis may be a local, layer-bounded phenomenon (e.g. fig. 6.14 of Hobbs *et al.* 1976) or occur pervasively in larger domains of crustal rocks. There are several mechanisms, each related to a different geodynamic setting, where fold–hinge-parallel stretching occurs, even on a large scale. One setting is related to collision zones which show evidence of oroclinal bending (Carey 1955, Ries & Shackleton 1976). Deformation in the outward arcs of oroclines involves a combination of thrust- and wrench-shear movements, causing fold-axis parallel extension (Coward & Potts 1983, Ridley 1986). On the other hand, extension parallel to the fold axis can also arise from early-stage thrusts that, after a change of shear direction, are overprinted by later thrusting and strike-slip movements (Ratliff *et al.* 1988, Dietrich 1989, Khudoley 1993). Other kinematic settings, associated with widespread development of fold axes parallel to the maximum stretching direction, are related to ductile shear zones in which simple shear is the dominant deformation type. Rotation of fold axes towards the direction of stretching (X-axis of the finite strain ellipsoid) is a common feature in simple shear regimes, which has been corroborated theoretically (Escher & Watterson 1974, Ramsay 1967, 1980, Hobbs *et al.* 1976, Skjernaa 1980, Jamison 1991) as well as by field observations (Wilson 1953, Lindstrom 1961, Bryant and Reed 1969, Sanderson 1973, Bell 1978, Williams 1978, Heitzmann 1987, Rajlich 1987). Fletcher & Bartley (1994) interpret folds with axes parallel to the stretching direction in ductile shear zones, to involve an additional shortening parallel to the Y-axis of the finite strain ellipsoid during shearing.

Sheath folds, with axes parallel to the stretching direction, develop by passive amplification of deflections in simple shear regimes with very high strain (e.g. Cobbold & Quinquis 1980, Malavieille 1987, Skjernaa 1989). Apart from sheath folds, passive amplification of pre-existing folds may also result in fold-axis parallel extension, provided that the amplitudes of the folds vary along strike. Since the growth rate of a fold increases with the amplitude during amplification (Biot 1961, Sherwin & Chapple 1968), high-amplitude folds will amplify much faster than small-amplitude folds causing hinge-parallel extension (see also Dietrich 1989). Transtension (in the sense of Harland 1971) is another potential deformational environment suitable for the growth of folds with their axes parallel to the principal stretching direction. Transtension regimes are characterized by overall prolate fabrics (Sanderson & Marchini 1984, Fossen & Tikoff 1993).

As an alternative to the conditions so far described, stretching parallel to the fold axes may occur under bulk plane strain without the necessity of extensive rotation of the initial fold axes, if the Y-axis of the finite strain ellipsoid is oriented perpendicular to the competent layers. This kinematic environment has been applied by Ramberg (1959), Watkinson (1975) and Grujic & Mancktelow (1993) to model fold-axis parallel stretch under plane strain conditions. Suitable prerequisites for this type of fold formation are a steeply inclined com-

petent layering and lateral extension. Stünitz (1991) and Froitzheim (1992) used this kinematic framework in order to interpret fold-axis parallel stretching lineations in the Western Alps.

Plane-strain folding, with the competent layer perpendicular to the principal stretching direction, can cause finite hinge-parallel extension if the layer suffered earlier flattening strain due to compaction (Treagus & Treagus 1981, Mazzoli & Carnemolla 1993).

Finally, pure constrictional strain conditions have to be considered as a potential kinematic configuration for the simultaneous formation of folds and stretching lineation, in which the fold axes are strictly parallel to the direction of extension. As under these conditions the bulk strain is coaxial, it should be possible to infer directions of regional principal stress from the fold geometry (Hudleston & Lan 1993 and references therein). In the following we present experimental results of such constrictional folding with the layering originally oriented parallel to the principal stretching direction.

PROCEDURE

A shear cylinder, made of PVC, was used to carry out the constrictional strain experiments. This cylinder was cut longitudinally on one side. It was loaded with a cylinder of layered plasticine which was lubricated with *Vaseline* on the outside to reduce the boundary interactions between the plasticine specimen and the inner wall of the shear cylinder. The undeformed plasticine specimen and the shear cylinder are shown in Figs. 1a and 2a, respectively. To decrease the diameter of the cylinder and consequently stretch the plasticine layers, a set of pipe fittings, wrapped around the shear cylinder, were slowly but constantly tightened to produce a strain rate of 8×10^{-3} s^{-1}. To prepare the plasticine specimens, another PVC-tube with the same diameter as the shear cylinder was cut into two halves (Fig. 2a). After lubricating the inner walls of the half cylinders with *Vaseline*, they were filled with plasticine. The two half-cylindrical bodies of plasticine were then extracted and fitted together to form a plasticine cylinder.

White and red modeling plasticine, produced by Weible KG (Schorndorf, Germany) was used. Originally, both have identical apparent viscosities. The apparent viscosity of the white plasticine was reduced by an addition of oil under heat (incompetent matrix). The resulting emulsion was homogenized by thorough mixing. As both types of plasticine are non-Newtonian materials (e.g. McClay 1976), their stress exponent (n), a material property in the flow law [see equation (1)] and their apparent viscosity (η) were determined based on the results of uniaxial compression tests carried out on a triaxial testing apparatus built by E. Aulbach at the Institut für Geophysik, University of Frankfurt a.M. Eight runs, each at different but constant strain rates, were performed at 20°C on plasticine cylinders (3 cm in height and diameter) up to a strain of 7%. Strain and stress were automatically recorded every 3 s.

The initial dimensions of the specimens used in the constrictional experiments were 100 mm in length and 45 mm in diameter. The initial thickness of the competent layer was varied in different runs. In order to provide an

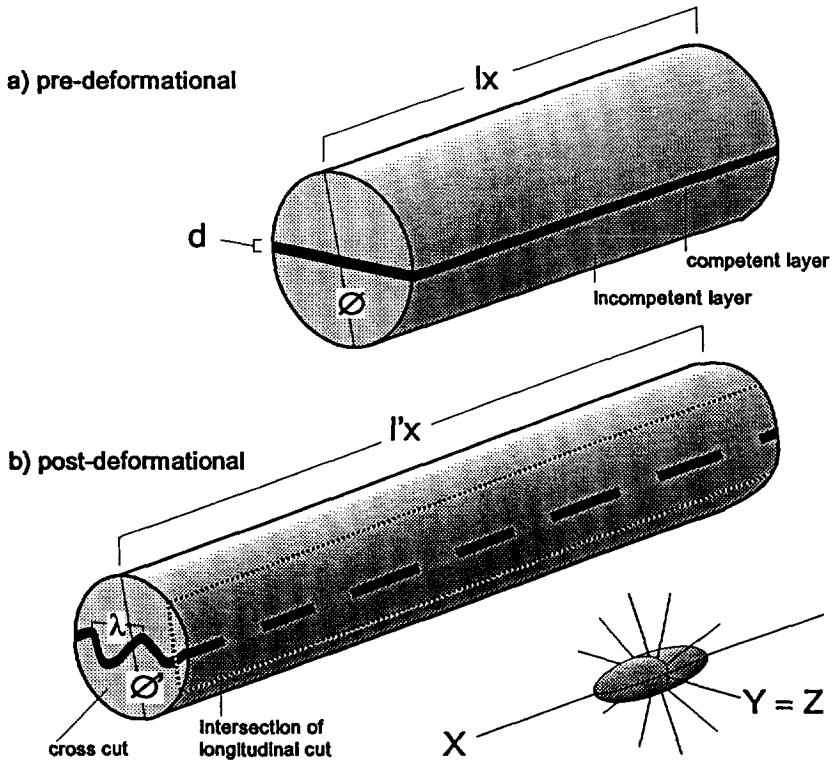

Fig. 1. Schematic illustration of the general aspects of a layered plasticine specimen before (a), and after (b) the constrictional deformation. The black layer represents the competent plasticine bed.

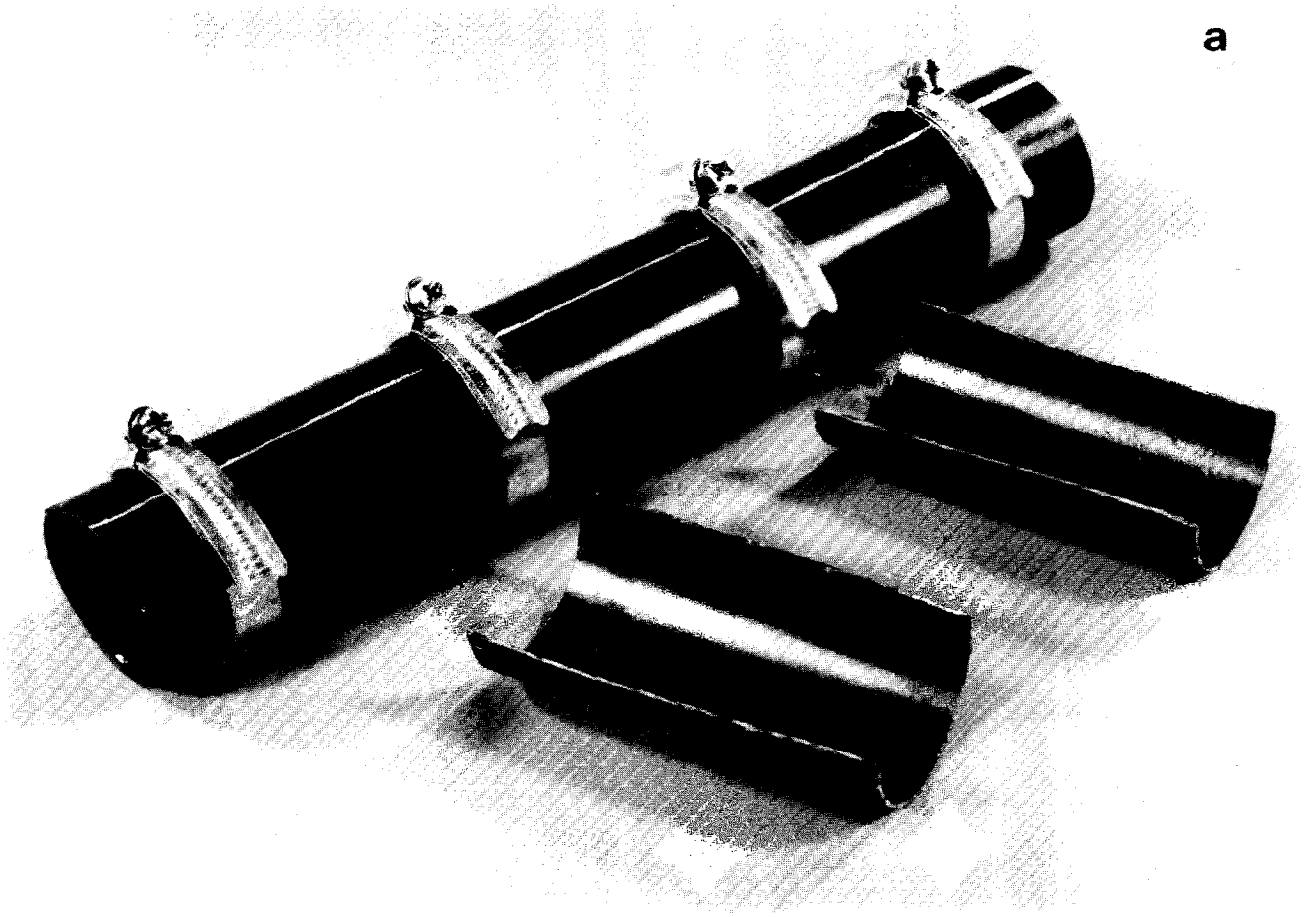

Fig. 2. (a) Longitudinally cut shear cylinder with pipe fittings. The two shorter half-cylinders (10 cm in length) were used to prepare the layered plasticine specimen. (b) Cross-cuts and (c) longitudinal cuts of selected specimens (of initially different layer thickness) after constriction. Note the average decrease in wavelength (cross cuts) and increasing number of boudins (longitudinal cuts) with decreasing initial layer thickness. Irregular low-amplitude folding, visible in longitudinal cuts, results from interaction of the specimens with the walls of the PVC-cylinder.

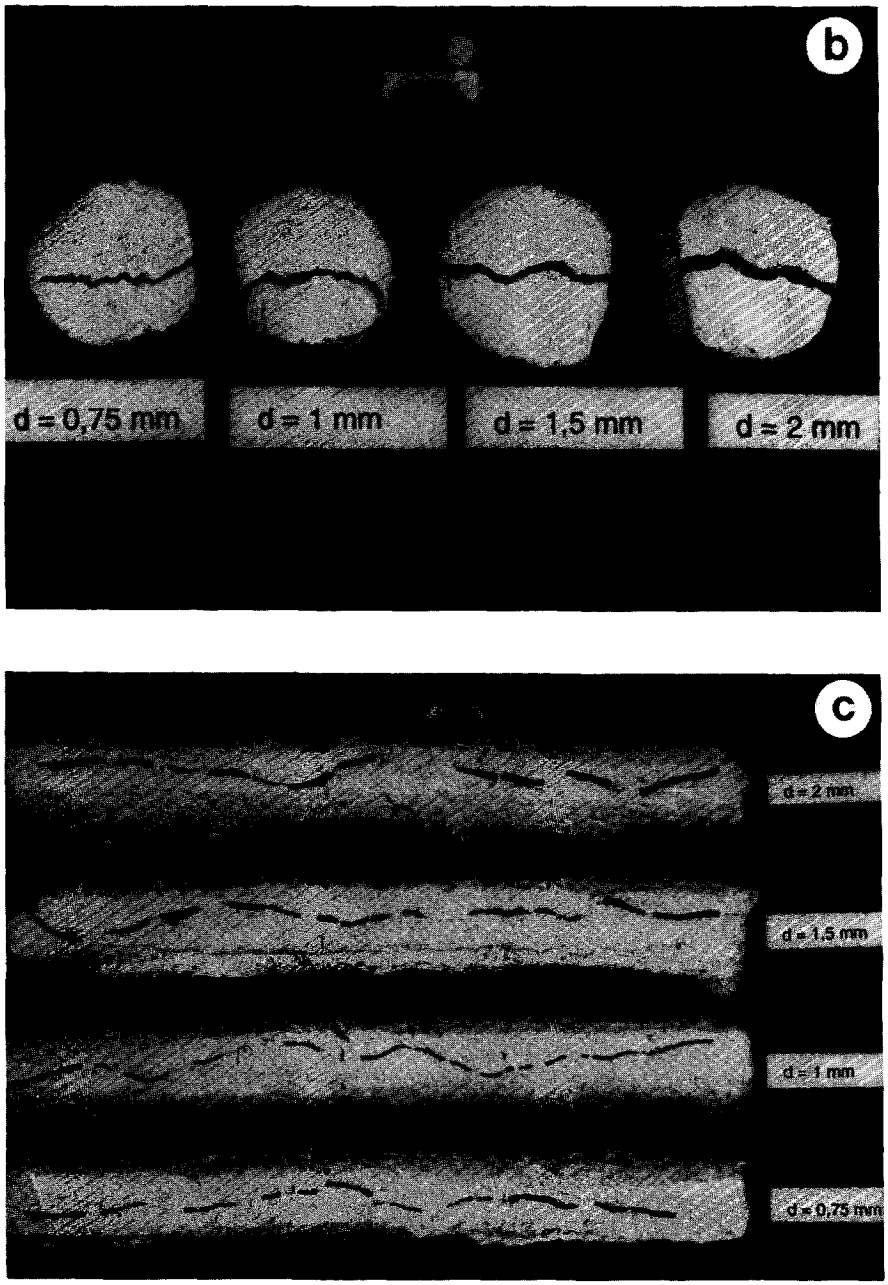

Fig. 2. *continued.*

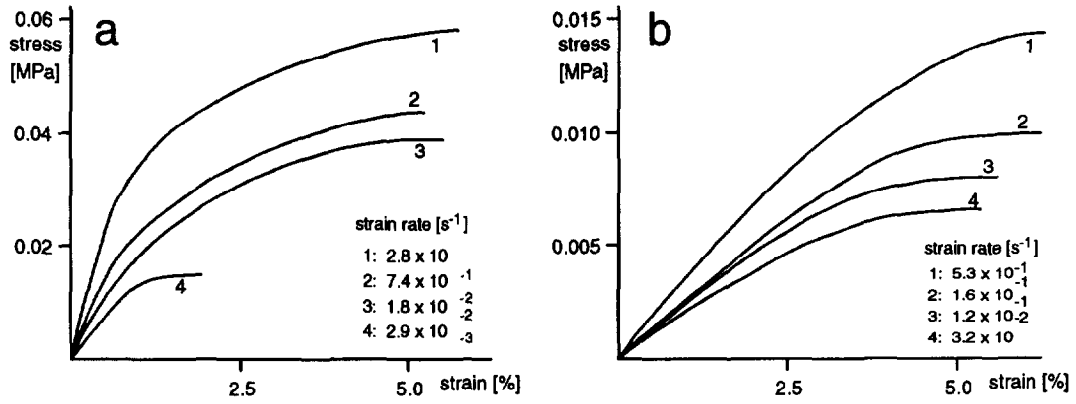

Fig. 3. Stress–strain curves for uniaxial compression tests on plasticine. All curves are corrected for machine loading characteristics and changes in specimen dimensions with strain. (a) Red, competent plasticine; (b) white, incompetent plasticine.

even and consistent geometry, the thin layer was prepared by the use of a hydraulic press. Figure 1 schematically illustrates the geometrical characteristics of a specimen before and after the deformation.

RESULTS

Stress exponents and apparent viscosities

The results of the uniaxial compression tests are shown in Fig. 3. The stress–strain plots indicate poorly defined yield transitions from elastic to plastic behavior at a strain of less then 5%. At a constant temperature and strain the constitutive flow law for plasticine reduces to the form:

$$\dot{\varepsilon} = C\,\sigma^n, \tag{1}$$

where $\dot{\varepsilon}$ is the strain rate, C is a temperature and strain dependent constant, σ is the applied stress, and n is the stress exponent (McClay 1976). Assuming steady-state flow and taking the stress at 5% strain, a plot of log strain rate vs log flow stress gives a straight line of slope n (Fig. 4). From this, n is determined to be 3.4 for the white and 7.2 for the red plasticine. As both n and C are known (Fig. 4), the apparent viscosity (η) can be calculated. Supposing that σ_0 is a reference stress (e.g. 0.01 MPa), the related strain rate ($\dot{\varepsilon}_0$) can be determined as

$$\dot{\varepsilon} = C\,\sigma_0^n. \tag{2}$$

The apparent viscosity can now be calculated using the equation

$$2\eta = \sigma/\dot{\varepsilon} = \sigma/\dot{\varepsilon}_0(\dot{\varepsilon}/\dot{\varepsilon}_0)^{(1-n)/n}, \tag{3}$$

where $\dot{\varepsilon}$ is the strain rate used in the constrictional experiments ($8 \times 10^{-3}\ s^{-1}$). Accordingly, the apparent viscosity (at 5% strain and a strain rate of $8 \times 10^{-3}\ s^{-1}$) is 2.17×10^6 Pa's for the red plasticine (η_1) and 2.34×10^5 Pa's for the white plasticine (η_2).

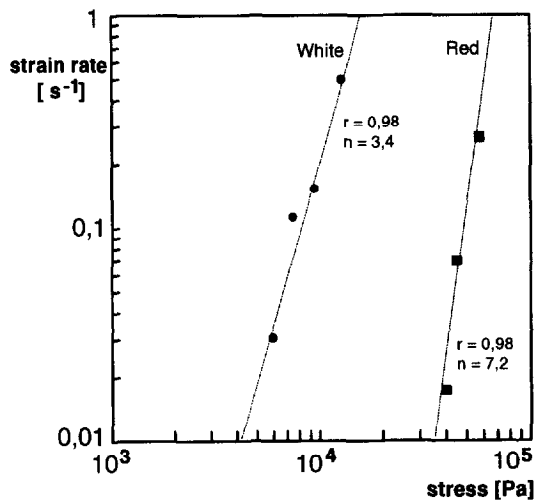

Fig. 4. Plots of log stress vs log strain rate (at 5% strain). Straight lines are best fits from a least squares regression analysis. r = Coefficient of correlation, n = derived stress (power-law) exponent. For further explanation see text.

Constrictional deformation

The volume of the specimens did not significantly change during the constrictional deformation. All sections, cut perpendicular to the stretching axis, show folding of the competent layers (Fig. 2b). All competent layers are boudinaged, as shown by sections cut parallel to the stretching axis (Fig. 2c). Low amplitude/large wavelength folding, seen in the latter sections, is restricted to the marginal parts of the specimens (< 1 cm). These effects are hardly visible on longitudinal cuts that halve the cylinder. This suggests that these deflections resulted from weak boundary interactions. Moreover, if plasticine of different color but identical viscosity is used to perform the constrictional experiments with the same layer orientation as described above, low amplitude/large wavelength folding is also observed at the marginal parts of the cylinders. As expected, cross cuts (YZ-plane) in these cases do not show folding.

The results of the experiments, documented in Table 1, are based on averaged data from measurements of several cross and longitudinal cuts. The amount of extension (e_x) is 1.4 for all specimens (I, Ia, II, IIa, III, IIIa, IV). Runs Ia, IIa and IIIa were carried out to show the reproducibility of particular configurations. The following finite parameters of the deformed specimens were measured: bulk length (l'_x), diameter (ϕ'), thick-

Table 1. Pre- and post-deformational data of various parameters in the experiments. l_x = Initial (pre-deformational) length of specimen, l'_x = final (post-deformational) length of specimen, e_x = bulk finite extension parallel to X of specimen, ϕ = initial diameter of specimen, ϕ' = final diameter of specimen, d = initial thickness of competent layer, d' = final thickness of competent layer, $l_{x(\text{neck})}$ = length of necks parallel to X, $l_{x(\text{boudin})}$ = sum of boudin lengths parallel to X, n_{boudin} = number of boudins, e_{1x} = finite ductile extension of competent layer parallel to X, W_a = average fold wavelength in cross cuts, and W_d = average wavelength/thickness

RUN	l_x (mm)	l'_x (mm)	e_x	ϕ (mm)	ϕ' (mm)	d (mm)	d' (mm)	$l_{x(\text{neck})}$ (mm)	$l_{x(\text{boudin})}$ (mm)	n_{boudin}	e_{1x}	W_a (mm)	W_d
I	100	240	1.4	45	29	2	2	59	181	8	0.81	11.2	5.6
Ia	100	240	1.4	45	29	2	2	75	165	12	0.65	12	6
II	100	240	1.4	45	29	1.5	1.5	68	172	11	0.72	7.5	5
IIa	100	240	1.4	45	29	1.5	1.5	68	172	15	0.72	8	5.3
III	100	240	1.4	45	29	1	1	70	170	17	0.7	6.2	6.2
IIIa	100	240	1.4	45	29	1	1	84	156	21	0.56	5.6	5.6
IV	100	240	1.4	45	29	0.75	0.75	86	156	16	0.56	4.7	6.3

ness of the competent layer (d'), sum of boudin lengths $l_{x\ \text{boud}}$) and number of boudins (n_{boud}). From this data base the finite, plastic, X-parallel elongation (boudinage excluded) of the red, competent layer (e_{1x}) was determined (Fig. 5c). The total arc length of the folds was measured in the manner described by Sherwin & Chapple (1968). The average wavelength (W_a) was calculated by the equation:

$$W_a = \text{total arc length}/n_{\text{fold}}, \quad (4)$$

where n_{fold} is the number of folds of the folded layer on the YZ-plane. This wavelength (W_a) is nearly the same as the initial wavelength (W_i *sensu* Ramsay & Huber 1987, p. 383) because the amplitude of the experimental folds is relatively low (W_a/average amplitude > 8). Buckling theory predicts a dominant wavelength/thickness, L_d (e.g. Hudleston & Lan 1993 and references therein), and it has been shown by Fletcher & Sherwin (1978) that the average value of wavelength/thickness, W_d, is a good estimate for L_d under conditions likely to hold for rocks. Therefore the value of W_d was determined for each run.

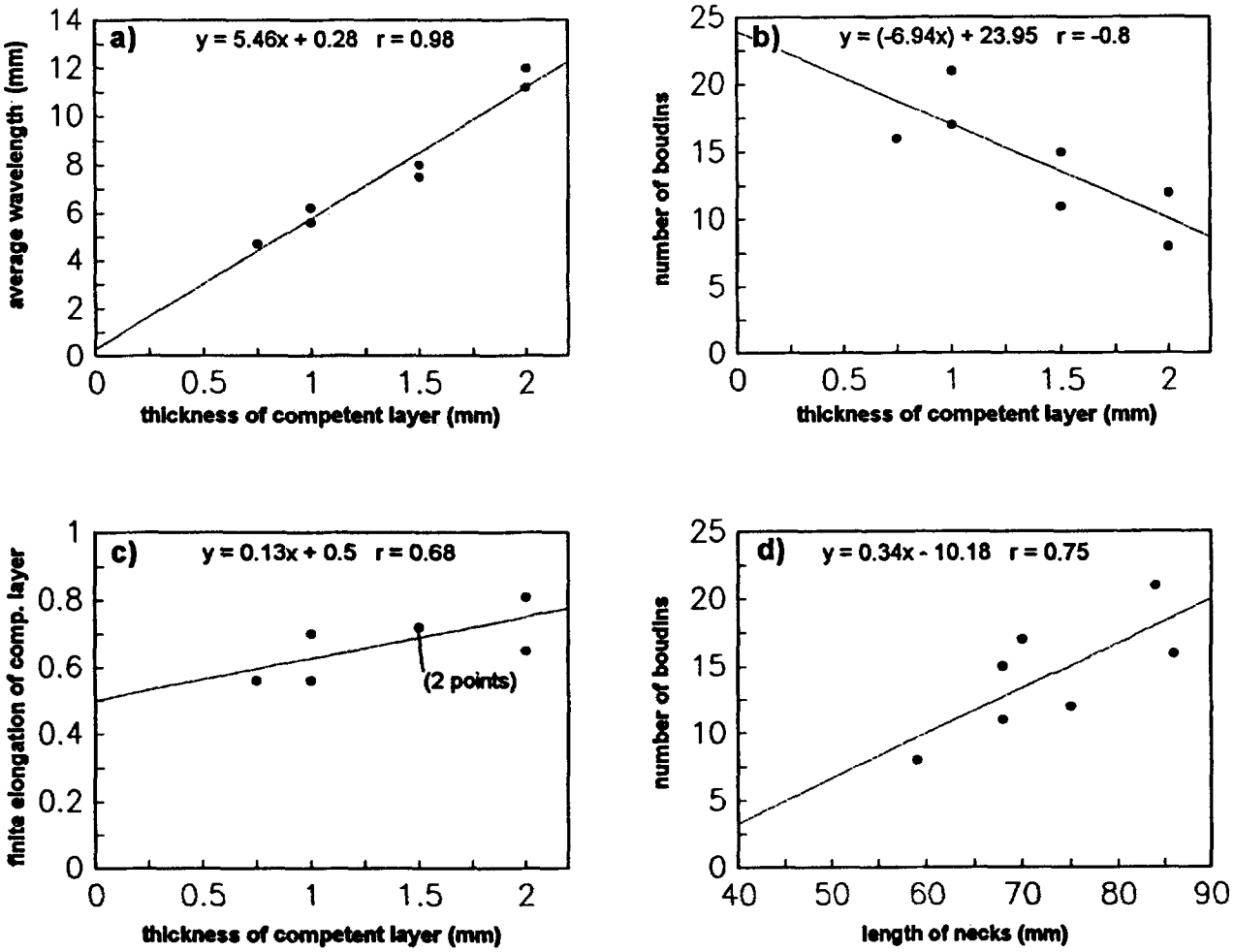

Fig. 5. (a)–(d) Diagrams showing the major results of the experiments. Functions and correlation coefficient, r, are represented at the top of each chart.

The data show that folds with axes parallel to the stretching direction generally develop under pure constrictional strain conditions. In all runs folding was accompanied by boudinage and plastic elongation parallel to the direction of principal extension. Boudinage appears to have developed from pinch- and swell-structures. Apparently, the thickness of the competent layer did not visibly change during deformation (Table 1), although the total arc length of the folded layer in YZ-sections (cross cuts) of each run decreased significantly (25%). The area of the incompetent white matrix in this section decreased by 60% whereas the area of the folded layer decreased by 30%.

The average wavelength (W_a), determined by equation (4), increased from 5 to 12 mm with increasing layer thickness (Fig. 5a). The wavelength/thickness ratio (W_d) of all runs is almost the same, ranging from 5.0 to 6.3 with an average value of 5.7 ± 0.4 (Table 1). The number of boudins (n_{boud}) declined from 21 to 8, with increasing layer thickness (Fig. 5b) and an associated decrease of neck lengths (Fig. 5d). It is further observed that the finite plastic elongation of the folded layer (e_{1x}) slightly increased, from 0.56 to 0.81, with layer thickness (Fig. 5c).

DISCUSSION

A striking feature of the experiments is the fact that the layer thickness did not change significantly throughout the procedure although the layer was remarkably shortened in the YZ-plane (Table 1). In order to maintain the principle of volume-constancy, the associated area decrease of the competent layer (in YZ) has to be compensated by adequate plastic elongation parallel to X (expressed by e_{1x} in Table 1). The difference in area decrease (in YZ) of the white matrix (60%) and the competent red layer (30%) seems to be directly related to the boudinage of the latter in the X-direction. The stronger area decrease of the matrix in cross cuts (YZ) is best envisaged as a filling of the gaps between the boudins of the competent layer during the constriction.

The wavelength/thickness ratio (W_d) is within the range described from natural folds (4–6; Sherwin & Chapple 1968). Similar values of W_d should also be expected applying the equation of Smith (1977, 1979), developed for the plane strain folding of power-law materials:

$$L_d \approx 3.46\,(n_2^{1/6}/n_1^{1/3})(\eta_1/\eta_2)^{1/3}, \qquad (5)$$

where n_1 and n_2 are the power-law exponents in the flow laws for layer and matrix, respectively. Substituting into equation (5) the measured values of the power-law exponents and the apparent viscosities, the dominant wavelength/thickness, L_d, is found to be 4.6. This is similar to the value of 5.7 found in the experiments for W_d. Thus the equation of Smith (1977, 1979) holds approximately also for folds formed under constrictional strain conditions.

Three-dimensional folding of an embedded viscous layer under pure shear has been investigated by Fletcher (1991). From his study, folding seems to be impossible under pure constriction. However, the material of the folded layer in Fletcher's model is of linear viscous (Newtonian) behavior. According to Smith (1977) Newtonian material cannot boudinage. Therefore, Fletcher's model is not suitable to explain folding and associated boudinage of an embedded layer of power-law behavior under pure constriction.

The fact that the plastic elongation of the folded layer parallel to X varies with layer thickness complicates the mathematical approximation for the given configuration. Plastic elongation decreases slightly with declining layer thickness (Fig. 5c). This trend is associated with an increasing number of boudins and increasing neck length (Fig. 5b) (see also Woldekidan 1982). The thinner the competent layers are, the higher their tendency to boudinage. This probably results from higher mechanical instabilities and reduced tensile strengths of thin layers compared to thicker ones. It is thus suggested that an increasing number of boudins, the necks of which can extend more easily than the boudins themselves, compensates for the loss in bulk finite plastic elongation of the thinner layers.

The observed development of constrictional folds is probably not restricted to experiments. Several natural deformational environments are thought to provide conditions necessary to produce true constrictional folds:

(1) The prolate strain configurations within the stems of salt diapirs are suitable for the formation of constrictional folds. Numerous examples of steeply plunging folds have been described from the interiors of salt diapirs (Talbot & Jackson 1987 and references therein). Concerning many salt diapirs in northern Germany, these folds have been termed 'Kulissenfalten' (curtain folds). Talbot & Jackson (1987) explained the formation of curtain folds by constrictional refolding of recumbent and sheath folds after their ascent and rotation into the stem of the diapir.

(2) A zone of constrictional strain is also conceivable in between several contemporary rising magmatic diapirs (Brun *et al.* 1981, Dixon & Summers 1983, Jelsma *et al.* 1993, Miller & Paterson 1994).

(3) Concerning metamorphic rocks, constrictional folds in eclogite-facies rocks have been described from the Western Gneiss Region of the Norwegian Caledonides (Andersen *et al.* 1991) and from the Western Alps (Henry *et al.* 1993).

CONCLUSIONS

Pure constriction seems to be a suitable environment for producing folds and boudins in power-law materials, provided the competent layer is oriented parallel to the principal stretching direction. Fold-axis parallel stretch is accommodated by boudinage and plastic elongation of the folded layer. Supposing this stretch is entirely plastic, and boudinage along the direction of principal extension is excluded, the difference in the apparent

viscosities is likely to be too small to initiate folding. Therefore, it is suggested that folding under these configurations is always associated with boudinage of the folded competent layer. Future investigations should focus on the relation between folding and associated boudinage during pure constrictional deformation, especially addressing the question of whether this type of folding is possible in Newtonian material in which boudinage is not possible.

Although it is often difficult to clearly recognize such folds in the field, the experimental results may help in their identification. Apart from boudinage, a further characteristic feature of these folds should be strict coaxial fabrics. The occurrence of a preferred fold vergence as well as planar fabrics (e.g. axial plane cleavage) would exclude a pure constrictional origin.

Acknowledgements—We thank L. Skjernaa, D. Grujic, P. J. Hudleston, P. Leat, R. Lisle, O. Oncken, H.-U. Schmincke, and an unknown reviewer for their discussion, constructive criticism, and reviews on the manuscript. The rheological parameters of the plasticine were determined by the second author G. Zulauf; J. Zinke kindly helped him to carry out the uniaxial compression tests, and G. Borm gave advice for the calculations of the viscosities. Both are gratefully acknowledged. G. Kobberger held a Ph.D.-grant from the Studienstiftung des Deutschen Volkes, and G. Zulauf is funded by the Deutsche Forschungsgemeinschaft [Zu 73/1-1].

REFERENCES

Andersen, T. B., Jamtweit, B., Dewey, J. F. & Swensson, E. 1991. Subduction and eduction of continental crust: major mechanisms during continent–continent collision and orogenic extensional collapse, a model based on the south Norwegian Caledonides. *Terra Nova* **3**, 303–310.

Bell, T. H. 1978. Progressive deformation and reorientation of fold axes in a ductile mylonite zone: the Woodroffe thrust. *Tectonophysics* **44**, 285–320.

Biot, M. A. 1961. Theory of folding of stratified viscoelastic media and its implications in tectonics and orogenesis. *Bull. geol. Soc. Am.* **72**, 1595–1620.

Brun, J. P., Gapais, D. & Le Theoff, B. 1981. The mantled gneiss dome of Kuopio (Finland): interfingering diapirs. *Tectonophysics* **74**, 283–304.

Bryant, B. & Reed, J. C. 1969. Significance of lineation and minor folds near major thrust faults in the southern Appalachians and the British and Norwegian Caledonides. *Geol. Mag.* **106**, 412–429.

Carey, S. W. 1955. The orocline concept in geotectonics. *Proc. R. Soc. Tasmania* **89**, 255–288.

Cobbold, P. R. & Quinquis, H. 1980. Development of sheath folds in shear regimes. *J. Struct. Geol.* **2**, 119–126.

Coward, M. P. & Potts, G. J. 1983. Complex strain patterns developed at the frontal and lateral tips of shear zones and thrust zones. *J. Struct. Geol.* **5**, 383–399.

Dietrich, D. 1989. Fold-axis parallel extension in an arcuate fold- and thrust belt: the case of the Helvetic nappes. *Tectonophysics* **170**, 183–212.

Dixon, J. M. & Summers, J. M. 1983. Patterns of total and incremental strain in subsiding troughs: experimental centrifuged models of inter-diapir synclines. *Can. J. Earth Sci.* **20**, 1843–1861.

Escher, A. & Watterson, J. 1974. Stretching fabrics, folds and crustal shortening. *Tectonophysics* **22**, 223–231.

Fletcher, J. M. & Bartley, J. M. 1994. Constrictional strain in a non-coaxial shear zone: implications for fold and rock fabric development, central Mojave metamorphic core complex, California. *J. Struct. Geol.* **16**, 555–570.

Fletcher, R. C. 1991. Three-dimensional folding of an embedded viscous layer in pure shear. *J. Struct. Geol.* **13**, 87–96.

Fletcher, R. C. & Sherwin, J. 1978. Arc lengths of single layer folds: a discussion of the comparison between theory and observations. *Am. J. Sci.* **278**, 1085–1098.

Fossen, H. & Tikoff, B. 1993. The deformation matrix for simultaneous simple shearing, pure shearing and volume change, and its application to transpression–transtension tectonics. *J. Struct. Geol.* **15**, 413–422.

Froitzheim, N. 1992. Formation of recumbent folds during synorogenic crustal extension (Austroalpine nappes, Switzerland). *Geology* **20**, 923–926.

Grujic, D. & Mancktelow, N. 1993. Folds with axes parallel to the extension direction. *Terra abstracts, Abstract supplement No. 12 to Terra Nova* **5**, 304.

Harland, W. B. 1971. Tectonic transpression in Caledonian Spitzbergen. *Geol. Mag.* **108**, 27–42.

Heitzmann, P. 1987. Evidence of late Oligocene/early Miocene backthrusting in the central alpine 'root zone'. *Geodinamica Acta* **1**, 183–192.

Henry, C., Michard, A. & Chopin, C. 1993. Geometry and structural evolution of ultra-high-pressure and high-pressure rocks from the Dora–Maira massif, Western Alps, Italy. *J. Struct. Geol.* **15**, 965–981.

Hobbs, B. E., Means, W. D. & Williams, P. F. 1976. *An Outline of Structural Geology*. Wiley, New York.

Hudleston, P. J. & Lan, L. 1993. Information from fold shapes. *J. Struct. Geol.* **15**, 253–264.

Jamison, W. R. 1991. Kinematics of compressional fold development in convergent wrench terranes. *Tectonophysics* **190**, 209–232.

Jelsma, H. A. & van der Beek, P. A. 1993. Tectonic evolution of the Bindura–Shamva greenstone belt (northern Zimbabwe): progressive deformation around diapiric batholiths. *J. Struct. Geol.* **15**, 163–176.

Khudoley, A. K. 1993. Structural and strain analyses of the middle part of the Talassian Alatau ridge (Middle Asia, Kirgizstan). *J. Struct. Geol.* **15**, 693–706.

Lindstrom, M. 1961. Beziehungen zwischen kleinen Faltenvergenzen und anderen Gefügemerkmalen in den Kaledoniden Skandinaviens. *Geol. Rdsch.* **51**, 144–180.

Malavieille, J. 1987. Extensional shearing deformation and km-scale 'a'-type folds in a Cordilleran metamorphic core complex (Raft River Mountains, NW-Italy). *Tectonics* **6**, 423–448.

Mazzoli, S. & Carnemolla, S. 1993. Effects of the superposition of compaction and tectonic strain during folding of a multilayer sequence—model and observations. *J. Struct. Geol.* **15**, 277–291.

McClay, K. R. 1976. The rheology of plasticine. *Tectonophysics* **33**, T7–T15.

Miller, R. B. & Paterson, S. R. 1994. The transition from magmatic to high-temperature solid-state deformation: implications from the Mount Stuart batholith, Washington. *J. Struct. Geol.* **16**, 853–865.

Rajlich, P. 1987. Variszische duktile Tektonik im Böhmischen Massiv. *Geol. Rdsch.* **76**, 755–786.

Ramberg, H. 1959. Evolution of ptygmatic folding. *Norsk. geol. Tidsskr.* **39**, 99–152.

Ramsay, J. G. 1967. *Folding and Fracturing of Rocks*. McGraw-Hill, New York.

Ramsay, J. G. 1980. Shear zone geometry: A review. *J. Struct. Geol.* **2**, 83–99.

Ramsay, J. G. & Huber, M. I. 1987. *The Techniques of Modern Structural Geology, Vol. 2: Folds and Fractures*. Academic Press, London.

Ratliff, R., Morris, A. & Dodt, M. 1988. Interaction between strike-slip and thrust shear: deformation of the Bullbreen Group, central-western Spitsbergen. *J. Geol.* **96**, 339–349.

Ridley, J. 1986. Parallel stretching lineations and fold axes oblique to a shear displacement direction—a model and observations. *J. Struct. Geol.* **8**, 647–653.

Ries, A. C. & Shackleton, R. M. 1976. Patterns of strain variations in arcuate fold belts. *Phils. Trans. R. Soc. London* **A238**, 281–288.

Sanderson, D. J. 1973. The development of fold axes oblique to the regional trend. *Tectonophysics* **16**, 55–70.

Sanderson, D. J. & Marchini, W. R. D. 1984. Transpression. *J. Struct. Geol.* **6**, 449–458.

Sherwin, J. & Chapple, W. M. 1968. Wavelengths of single layer folds: a comparison between theory and observation. *Am. J. Sci.* **266**, 167–179.

Skjernaa, L. 1980. Rotation and deformation of randomly oriented planar and linear structures in progressive simple shear. *J. Struct. Geol.* **2**, 101–109.

Skjernaa, L. 1989. Tabular folds and sheath folds: definitions and conceptual models for their development, with examples from the Grapesvare area, northern Sweden. *J. Struct. Geol.* **11**, 689–703.

Smith, R. B. 1977. Formation of folds, boudinage and mullions in non-Newtonian materials. *Bull. geol. Soc. Am.* **88**, 312–320.

Smith, R. B. 1979. The folding of a strongly non-Newtonian layer. *Am. J. Sci.* **279**, 272–287.

Stünitz, H. 1991. Folding and shear deformation in quartzites, inferred from crystallographic preferred orientation and shape fabrics. *J. Struct. Geol.* **13**, 71–86.

Talbot, C. J. & Jackson, M. P. A. 1987. Internal kinematics of salt diapirs. *Bull. Am. Ass. Petrol. Geol.* **71**, 1086–1093.

Treagus, J. E. & Treagus, S. H. 1981. Folds and strain ellipsoid: a general model. *J. Struct. Geol.* **3**, 1–17.

Watkinson, A. J. 1975. Multilayer folds initiated in bulk plain strain, with the axis of no change perpendicular to the layering. *Tectonophysics* **28**, T7–T11.

Williams, G. D. 1978. Rotation of contemporary folds into the x-direction during overthrust processes in Laksefjord, Finnmark. *Tectonophysics* **48**, 29–40.

Wilson, G. 1953. Mullion and rodding structures in the Moine Series of Scotland. *Proc. Geol. Ass.* **64**, 118–151.

Woldekidan, T. 1982. Deformation of multilayers compressed normal to layering. Unpublished Ph.D. Thesis, University of London.